JOURNAL OF GEOPHYSICAL RESEARCH, VOL. 112, D16111, doi:10.1029/2006JD008346, 2007

Diurnal cycle of precipitation in the NASA Seasonal to Interannual Prediction Project atmospheric general circulation model

Myong-In Lee,[1,2] Siegfried D. Schubert,[2] Max J. Suarez,[2] Thomas L. Bell,[2] and Kyu-Myong Kim[1,2]

Received 13 December 2006; revised 15 May 2007; accepted 14 June 2007; published 30 August 2007.

[1] The global statistics of the diurnal cycle of warm-season precipitation simulated by NASA's Seasonal to Interannual Prediction Project (NASA/NSIPP) atmospheric general circulation model (AGCM) were evaluated using the Tropical Rainfall Measuring Mission (TRMM) Microwave Imager (TMI) rain retrievals. The model has notable biases in the phase of the diurnal cycle over land, where it produces rainfall maxima in the early afternoon, several hours earlier than the observed evening maxima. The model also produces too little precipitation in the nighttime over land. Similar biases in the phase were found over ocean, although the statistics are less robust. An analysis of the convective and stratiform contributions to the precipitation indicates that the incorrect representation of the diurnal cycle is primarily tied to deficiencies in the deep convection scheme. A set of sensitivity experiments shows that the phase of the maximum diurnal precipitation is quite sensitive to the change of the convection starting (parcel origination) level and the increase of the convection adjustment (relaxation) timescale in the Relaxed Arakawa-Schubert scheme. Both modifications act to delay the timing for the maximum development of CAPE, which lead to improvements in the diurnal cycle of precipitation, especially in correcting the phase errors over land, although the modifications tend to reduce the diurnal amplitudes substantially. The study suggests that improvements to the diurnal cycle in current models require improvements to the parameterized deep convection schemes, including the coupling with the boundary layer, the characteristic timescale of convection adjustment, and the triggering process for nocturnal precipitation.

Citation: Lee, M.-I., S. D. Schubert, M. J. Suarez, T. L. Bell, and K.-M. Kim (2007), Diurnal cycle of precipitation in the NASA Seasonal to Interannual Prediction Project atmospheric general circulation model, *J. Geophys. Res.*, *112*, D16111, doi:10.1029/2006JD008346.

1. Introduction

[2] The diurnal cycle of precipitation exhibits substantial geographical variation in both its amplitude and phase in the warm season. These variations are for the most part poorly simulated by current regional and global climate models [e.g., *Dai et al.*, 1999; *Lin et al.*, 2000; *Yang and Slingo*, 2001; *Dai and Trenberth*, 2004; *Collier and Bowman*, 2004; *Liang et al.*, 2004; *Dai*, 2006; *Lee et al.*, 2007a, 2007b]. A typical problem is the too-early development of the diurnal maximum over continental land regions, which is several hours earlier than the observed late afternoon to evening maximum. Phase biases are also evident over the oceans, where the models tend to produce the nocturnal rainfall maximum after local midnight compared with the observed early morning maximum. On the other hand, the amplitude biases tend to be more model-dependent.

[3] A number of studies suggest that these deficiencies in the diurnal cycle are primarily the result of deficiencies in the parameterization of atmospheric convection and related processes. Although the coarse horizontal resolution of current climate models does not resolve the organized mesoscale convective systems, which are frequently observed in summertime and contribute to a distinct diurnal variation over some locations such as the U.S. Great Plains [*Riley et al.*, 1987; *Carbone et al.*, 2002; *Nesbitt and Zipser*, 2003], the model deficiencies in the diurnal cycle seem to be fairly systematic and are not entirely removed by an increase in resolution [*Lee et al.*, 2007b, hereinafter referred to as L07b].

[4] *Chen et al.* [1996] and *Dai et al.* [1999] suggest that the criteria for the onset of moist convection (or convection trigger) may be too weak so that moist convection starts too early and occurs too often, which is likely the reason for the early development of precipitation over the land. *Dai and Trenberth* [2004] argue that the weak criteria for convection prevents the convective available potential energy (CAPE) from being accumulated enough to trigger more intense convection later in the day. *Dai* [2006] found similar characteristics of the simulated precipitation from the

[1]Goddard Earth Sciences and Technology Center, University of Maryland Baltimore County, Baltimore, Maryland, USA.
[2]NASA Goddard Space Flight Center, Greenbelt, Maryland, USA.

0148-0227/07/2006JD008346$09.00

newest generation of coupled GCMs. In fact, the study showed that the models tend to underestimate the frequency for heavy (>20 mm day^{-1}) precipitation and overestimate the frequency for light (<10 mm day^{-1}) precipitation.

[5] The onset of convection is closely related to the temporal variation of convective instability, which is measured by CAPE in many models. For land convection, the diurnal variation of the planetary boundary layer (PBL) strongly affects the diurnal variation of CAPE. The large-scale variations of the free atmosphere can also affect the convective instability and seem to be more important over the ocean and certain land regions where the nocturnal precipitation dominates. For example, *Zhang* [2003] emphasized the importance of this mechanism to nocturnal precipitation maximum over the U.S. Great Plains. By eliminating the PBL forcing in a CAPE-type closure scheme, he found a substantial delay in the timing of the maximum precipitation. However, the modification resulted in precipitation maxima shifted to the nighttime over most of the continent [*Collier and Zhang*, 2006].

[6] *Lee et al.* [2007a, hereinafter referred to as L07a], on the basis of an analysis of three AGCMs, suggested that the coupling process between deep convection and the PBL could be important for determining the phase of the maximum precipitation. They noted that, by design, buoyancy (CAPE) closure schemes such as the Arakawa-Schubert [*Arakawa and Schubert*, 1974] or its variants may induce too much sensitivity to the ground and PBL variations, and this might explain the tendency to convect too early (around local noon). A detailed analysis of the NASA/NSIPP AGCM with the relaxed version of Arakawa-Schubert scheme (RAS [*Moorthi and Suarez*, 1992]) showed that the lifting of the convection starting level (i.e., origination level of the vertically lifted parcel) from the ground to a higher level acted to delay the maximum phase of the diurnal precipitation by several hours. They also found a similar tendency of phase delay when they increased the convection adjustment (relaxation) timescale of RAS. Their results suggest that both modifications could modify the onset of diurnal convection through modifying the diurnal variation of CAPE, although they do not provide a detailed analysis of the mechanism. Given that CAPE is a key parameter that many convection schemes rely on to produce precipitation, the question of how those modifications affect the diurnal variation of CAPE is of primary importance for understanding the sensitivity of the diurnal cycle to the convection scheme.

[7] Motivated by the study of L07a, this study examines in more detail the mechanisms for the diurnal cycle of precipitation and how the modifications in the convection scheme affect the simulated diurnal cycles of precipitation and CAPE using the NASA/NSIPP AGCM (the same model used in L07a). We also extend the L07a analysis of North America to the global domain, to help assess how the modifications impact the diurnal cycle in a wide range of land and ocean conditions. We validate the diurnal cycle of precipitation globally and regionally using the Tropical Rainfall Measuring Mission (TRMM) Microwave Imager (TMI) satellite rainfall measurements. In order to facilitate the comparison with the TRMM measurements, we have forced the AGCM with observed sea surface temperatures (SSTs) for the same time period that the TRMM measurements are available (1998–2004). CAPE and other aspects of the diurnal cycle are validated for selected regions where observations are available from several different field experiments.

[8] Specifically, this study will attempt to address the following questions: (1) What are the observed and simulated global characteristics of the diurnal cycle of warm-season precipitation? In particular, what are the model biases in land and oceanic precipitation? (2) How much is the convection parameterization responsible for those biases? (3) How sensitive is the diurnal cycle to the modifications in the convection scheme? (4) What are the detailed processes that drive those sensitivities in the model? We will also discuss more generally what we can hope to gain from such modifications to current convection schemes, as well as the fundamental limitations of this approach.

[9] In the next section, we begin by describing the observations, model experiments, and the analysis methods.

2. Observations and Model Experiments

2.1. TRMM Data

[10] The observed diurnal cycle of precipitation was derived from rainfall estimates made with the TRMM TMI. TRMM product 2A12, version 6 [e.g., *Kummerow et al.*, 2000; *Olson et al.*, 2006] consists of rainfall estimates for each instrument field of view in the TMI scanning area. On the basis of seven summer seasons of data for 1998–2004, the time sequence $R(t_i)$, $i = 1, \ldots, n$, of area-averaged rain rate for each 2.5° × 2.5° grid box was obtained, where t_i is the time of the ith overflight of the area by TRMM and A_i is the portion of the grid box observed. The sequence of area averages was then fit to a sum of two sinusoids representing diurnal and semidiurnal cycles,

$$R(t_i) = r_0 + r_1 \cos[\omega_1(ti - \phi_1)] + r_2 \cos[\omega_2(t_i - \phi_2)], \quad (1)$$

where r_0 is the mean rain rate, r_1 and ϕ_1 are the amplitude and phase of the diurnal cycle, with $\omega_1 = 2\pi/(24 \text{ hours})$, and r_2 and ϕ_2 are the amplitude and phase of the semidiurnal cycle, with $\omega_2 = 2\pi/(12 \text{ hours})$. The fitting procedure uses a generalized least squares approach by expanding the cosines to create an expression linear in $\cos(\omega_k t_i)$ and $\sin(\omega_k t_i)$. The statistical significance levels of the amplitudes r_1 and r_2 are estimated using a modification of the theory described by *Bell and Reid* [1993], where it is shown that the probability that an amplitude r_k exceeds a value r is given by $\exp(-r^2/\sigma^2)$ under the null hypothesis $r_k = 0$. The "noise" level σ is obtained from the estimated variance of the coefficients in the linearized version of (1), assuming that the time correlation of area-averaged rain rate is described by $\exp(-|t_i - t_j|/\tau)$ for $i \neq j$, with a decorrelation time τ = 6 hours as suggested by *Bell et al.* [2001]. Observations covering less than 10% of the grid box area are ignored, and contributions to the variance estimates from partial observations are empirically reduced on the basis of an assumed dependence of the variance of area-averaged rain rate on the area A_i (to which the estimates are not particularly sensitive). This study used TRMM precipitation estimates within latitudes 20°S–40°N where the diurnal

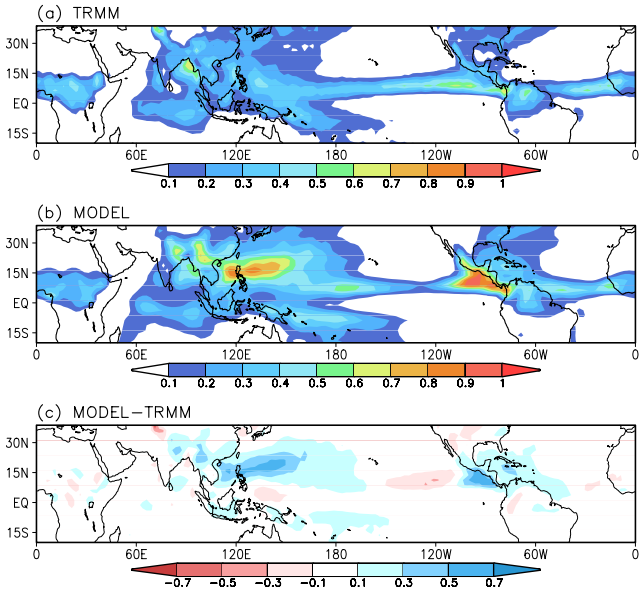

Figure 1. Summer mean (June–August) precipitation (mm h^{-1}) in (a) TRMM and (b) the AMIP simulation. (c) Difference between the AMIP run and TRMM.

variations are quite distinct in the Northern Hemisphere warm season.

2.2. Model Experiments

[11] The model is the NASA/NSIPP AGCM version 2 [*Bacmeister et al.*, 2000], which is the same model used in the intercomparison studies of L07a and L07b. It is a grid point model that incorporates the *Suarez and Takacs* [1995] dynamical core and a vertical sigma coordinate [*Arakawa and Suarez*, 1983]. The deep convection parameterization is based on the RAS scheme. The boundary layer/vertical diffusion is parameterized on the basis of a local diffusion scheme [*Louis et al.*, 1982]. The solar and infrared radiation schemes are from *Chou et al.* [1998] and *Chou and Suarez* [1994], respectively. The land surface model is the mosaic scheme developed by *Koster and Suarez* [1996].

[12] In order to facilitate the comparison with the observations, the model was integrated over a seven year period that begins with the availability of TRMM observations (1998–2004), forced by observed weekly SSTs and sea ice distributions [*Reynolds et al.*, 2002]. The model was run at a horizontal resolution of 2° latitude by 2.5° longitude (similar to the resolution of the TRMM precipitation data), and with 40 vertical levels. For convenience, this simulation is denoted as the AMIP (Atmospheric Model Intercomparison Project) run.

[13] Figure 1 compares the seasonal mean precipitation amounts from the TRMM observation with those from the AMIP simulation. The model tends to produce overall wet biases especially over the intertropical convergence zones (ITCZs) in the western and eastern Pacific. The model also produces excessive rainfall over land in the Indian-Asian monsoon region.

[14] In addition to analyzing the above-mentioned AMIP run, we will also further analyze the experiments conducted in L07a (these were actually redone for this study to save more output and with some differences as noted below) to assess the global impacts of the modifications to the convection scheme. These simulations, spanning only one season, were forced by climatological mean (1983–2002 average) SST to save computation time. However, as will be shown, the diurnal cycles are not qualitatively different.

[15] As described in L07a, we focus on two modifications to the RAS scheme consisting of changes in the convection starting level and the relaxation timescale. For the buoyancy calculation (equivalent to calculating CAPE with entrainment), the standard scheme uses the moist static energy (MSE) that is averaged over the lowest two model levels to provide the initial states of the lifted parcel. In the modified run (EXP1), the number of averaging levels was increased to include the lowest 10 levels, corresponding to a layer from the ground up to a pressure level of 0.85 times the surface pressure. This modification is intended to prescribe the PBL mean MSE to the lifted parcel.

[16] In EXP2, we increased the relaxation timescale from 30 min in the standard scheme to 12 hours. Although this timescale is frequently used as a free parameter for tuning the convection scheme, it can be thought of as the time over which the cloud effects would reduce the cloud work function (similar to CAPE) to its equilibrium value [*Moorthi and Suarez*, 1992]. This is regarded as different from the actual lifetime for individual cumuli, and represents the characteristic timescale of the overturning circulation driven by cumulus mass flux. This timescale should be dependent on cloud type (height), and typical values are of the order of 10^3–10^4 s [*Arakawa and Schubert*, 1974]. Given that range of values, the tested timescale of 12 hours is certainly on the long side, but it nevertheless suits our purpose of testing sensitivity. It should be noted that in these runs the timescale is independent of cloud height, which is slightly different from the runs described in L07a. This is a simpler modification to the standard scheme, although varying the relaxation timescale with cloud height also impacts the simulated diurnal cycle [*Lin et al.*, 2000].

[17] In EXP3, we tested the combined impact of changing the convection starting levels and the relaxation timescale. Those three sensitivity runs are compared with the control run (CTRL) with the standard scheme. Table 1 summarizes the experiments.

2.3. Validation

[18] In defining the amplitude and phase of the simulated diurnal cycle of precipitation, a mean 24-hour diurnal time series of precipitation was constructed by averaging precipitation amount hour by hour over the entire time period available. This time mean diurnal cycle was then decomposed using Fourier harmonic analysis to determine the amplitude and phase of the wave number 1 (24-hour cycle) and wave number 2 (12-hour) component. The significance tests for the estimated amplitude and phase of the diurnal cycle are described in L07b (see their appendix). A grid

Table 1. A Description of the Model Sensitivity Experiments

	Convection Starting Level	Relaxation Timescale, hours
CTRL	2 (σ = 0.98)	0.5
EXP1	10 (σ = 0.86)	0.5
EXP2	2 (σ = 0.98)	12
EXP3	10 (σ = 0.86)	12

Table 2. A Description of the Observed Sounding Data Sets Used in This Study

	Domain	IOPs	Interval, hours	Data Reference
NAME	22–35°N, 115–100°W, 1° × 1° gridded	7 Jul to 15 Aug 2004	6	*Johnson et al.* [2007]
ARM	averaged at 36.91°N, 97.49°W,	18 Jul to 4 Aug 1995, 18 Jun to 17 Jul 1997, 12 Jul to 22 Jul 1999	3	*Zhang et al.* [2001]
GATE	4–14°N, 19–28°W, 1° × 1° gridded	30 Aug to 18 Sep 1974	3	Colorado State University
TOGA COARE	Intensive Flux Array–averaged (5°S–5°N, 150–160°E)	1 Nov 1992 to 28 Feb 1993	6	*Ciesielski et al.* [2003]

point is considered to have a nonzero diurnal cycle if the values are significant at the 10% level. We focus on the first harmonic (24-hour cycle) that dominates the daily cycle at most grid points in the model simulation, and provides a useful way to calculate the maximum phase of the time mean diurnal cycle [*Dai et al.*, 1999; *Bowman et al.*, 2005; *Dai*, 2006]. The results from the harmonic analysis were not significantly changed when we calculated the maximum and the preferred time directly from the time series. We note that the semidiurnal cycle of the simulated precipitation is weak, and we do not consider it here.

[19] In order to validate vertical profiles of the MSE, we use the vertical sounding observations from four field experiments: the North American Monsoon Experiment (NAME), the Atmospheric Radiation Measurement Program (ARM), the Global Atmospheric Research Program's (GARP) Atlantic Tropical Experiment (GATE), and the Tropical Ocean Global Atmosphere Coupled Ocean Atmosphere Response Experiment (TOGA COARE). See Table 2 for a description of these data sets. Most of the Intensive Observing Periods (IOPs) occurred during the Northern Hemispheric summer except for TOGA COARE, but we do not expect significant differences in our diurnal cycle analysis. From those data sets, we constructed the IOP mean diurnal time series of MSE. The 1° × 1° gridded products from NAME and GATE were averaged over the domain, where we only used the land points in NAME and ocean points in GATE.

3. Comparisons Between TRMM and AMIP

3.1. Diurnal Cycle of Precipitation

[20] The amplitudes of the observed (TRMM) and simulated (AMIP) diurnal cycles of precipitation are compared in Figure 2. The model produces larger variability over the continents compared with the oceans, consistent with the TRMM observations. However, the amplitude biases are somewhat larger over the continents, where they show larger wet biases in the major precipitation regions. The bias patterns of the seasonal mean rainfall (Figure 1c) and the diurnal cycle amplitudes (Figure 2c) are similar over the continents, suggesting that the time mean biases are, in general, proportional to the amplitude biases in the diurnal cycle of precipitation.

[21] The amplitudes of the simulated diurnal cycle over the oceans are weak, again consistent with the observations. The model captures the regional characteristics of stronger signals over the adjacent oceans, such as the Bay of Bengal, the eastern Pacific, and the eastern Atlantic Oceans. In spite of large wet biases in the seasonal mean precipitation, the model simulates a realistic suppression of the diurnal variability over the western Pacific.

[22] Figure 3 compares the phase of the maximum in the diurnal cycle of precipitation between TRMM and the AMIP run, in terms of the local solar time (LST). The TRMM data show that over most of the continental regions the maxima occur between late afternoon and evening hours. The model shows noticeable phase biases over land, where it tends to simulate a maximum several hours earlier than observed. The TRMM data show nocturnal maxima (1800 to 0600 LST) on the southern flanks of the Tibetan Plateau, over the upper Amazonian basin, and over the U.S. Great Plains, which are poorly simulated by the model with large phase differences (Figure 3c). The lack of nocturnal precipitation is a common model deficiency, for example in the U.S. Great Plains [*Dai et al.*, 1999; *Zhang*, 2003; L07a; L07b]. Most of the oceanic regions exhibit maxima between just after midnight and early morning in the TRMM data. Although the phase biases over the oceans are less systematic (the signals are noisy in both the TRMM data and the AMIP run), it appears that the model precipitation maxima generally occur too early. The early phase biases are also evident in the adjacent oceans, although the model captures distinct signals of morning maxima that are consistent with the TRMM observations.

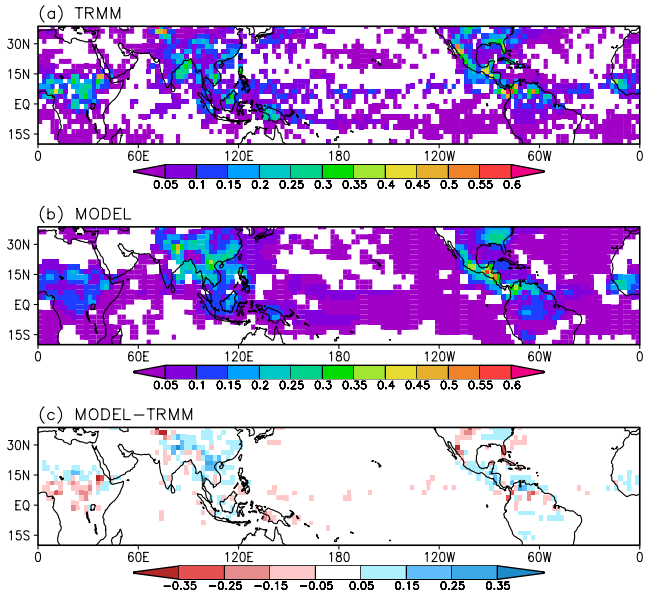

Figure 2. Amplitudes of the diurnal cycle of precipitation (mm h^{-1}) obtained from (a) TRMM and (b) the AMIP simulation. Only the grid points with an amplitude that is significant at the 10% level are shaded. (c) Difference between the simulation and the observation.

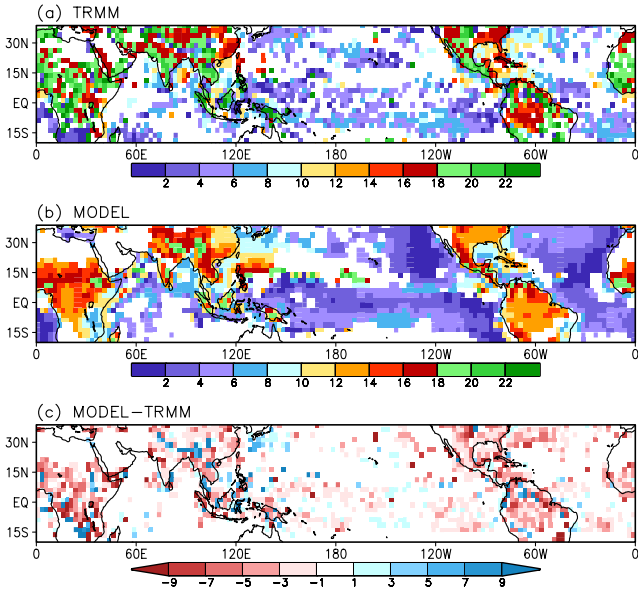

Figure 3. Same as in Figure 2 except the maximum phases of the diurnal cycle of precipitation indicated in local solar time (LST).

[23] In order to summarize the broad-scale signals of the diurnal cycle of precipitation over land and ocean, Figure 4 shows histograms of precipitation maxima for the land and ocean grid points as a function of LST. For that comparison, only those grid points with a statistically significant signal and where the diurnal cycle is defined in the TRMM observations were counted. This had a considerable impact on the probability distribution of peak times over ocean, but had little impact on the land statistics. In TRMM, the land precipitation maxima tend to occur around 1800 LST, with a weaker secondary peak around 0100 LST. On the other hand, the maxima in the simulation are concentrated around 1400 LST, which is about 4 hours earlier than TRMM. The model produces very little precipitation in the nighttime after 2200 LST. Oceanic phase biases are relatively small with a peak in the histogram at 0500 LST for TRMM and 0400 LST for AMIP, although the ocean statistics are sampled less well than the land statistics.

3.2. Convective Versus Stratiform Precipitation

[24] The model simulations are examined further by separating the convective (CNV) and stratiform precipitation (large-scale condensation, hereinafter LSC). We find that the model simulates a large CNV ratio in total precipitation (greater than 70%) in most of the major precipitation regions. The ratio is even higher in the tropical ITCZ regions, where it gets as high as 95%. This is in contrast to the TRMM observations, which indicate that over the tropical oceans, stratiform precipitation is comparable (45–55%) to the convective precipitation [*Schumacher and Houze*, 2003]. *Dai* [2006] indicates that the dominance of convective over stratiform precipitation is common in current GCMs.

[25] Figure 5 compares the amplitudes and phases of the CNV and LSC diurnal cycles. Over most parts of the continents, the amplitude of the LSC diurnal cycle (Figure 5b) is much smaller that that of CNV (Figure 5a). The maximum phases of the CNV diurnal variations (Figure 5c) tend to resemble those of the total precipitation in most continental areas (Figure 3b). This suggests that the convection scheme is primarily responsible for the phase biases. Over those regions, the LSC precipitation maximum occurs at local nighttime, which is delayed by several hours or even out of phase with the CNV maximum.

[26] The dominance of CNV precipitation in the diurnal cycle amplitudes is also evident in most of the oceanic regions. However, this relation is not true in the western Pacific, where the model produces strong wet biases in the seasonal mean. The amplitude of the diurnal CNV precipitation is small and, for the most part, the peak phases are not significant over this region. Instead, late afternoon peaks of LSC precipitation are prominent. Over this region, we notice that the CNV ratio is higher than 70%, suggesting that the CNV precipitation is contributing to the time mean wet biases randomly in time with respect to the diurnal cycle.

4. Sensitivity to the Modifications in the Convection Scheme

4.1. Changes in the Diurnal Cycle of Precipitation

[27] In this section, we examine the sensitivity of the diurnal cycle to modifications in the convection scheme. We begin by examining the impact on the seasonal mean precipitation (Figure 6). The precipitation patterns from the control (CTRL) run forced with climatological SSTs are not much different from the multiyear averaged precipitation patterns from the AMIP run (compare Figure 1b). To a large extent, the model biases change little among the sensitivity runs, though EXP3 (Figure 6d) has reduced wet biases in the western and eastern Pacific ITCZs.

[28] We next compare the simulated amplitudes and maximum phases of the diurnal cycle of precipitation

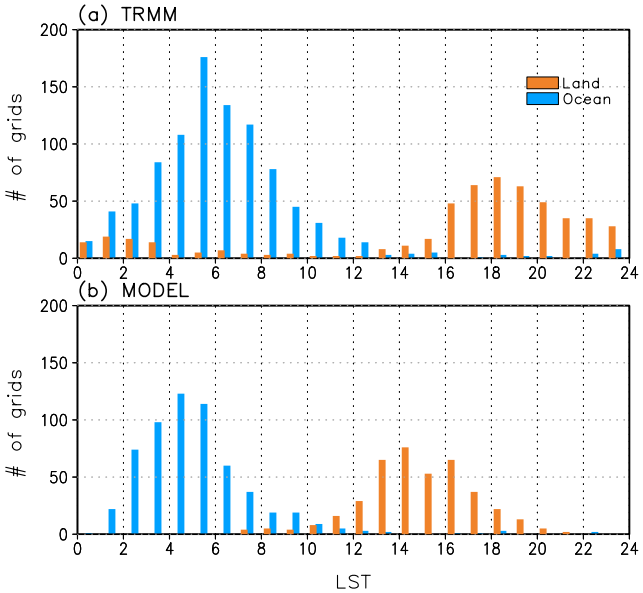

Figure 4. Histograms of the maximum phases in the diurnal cycle of precipitation in the land and ocean grid points appearing in (a) TRMM and (b) the AMIP simulation.

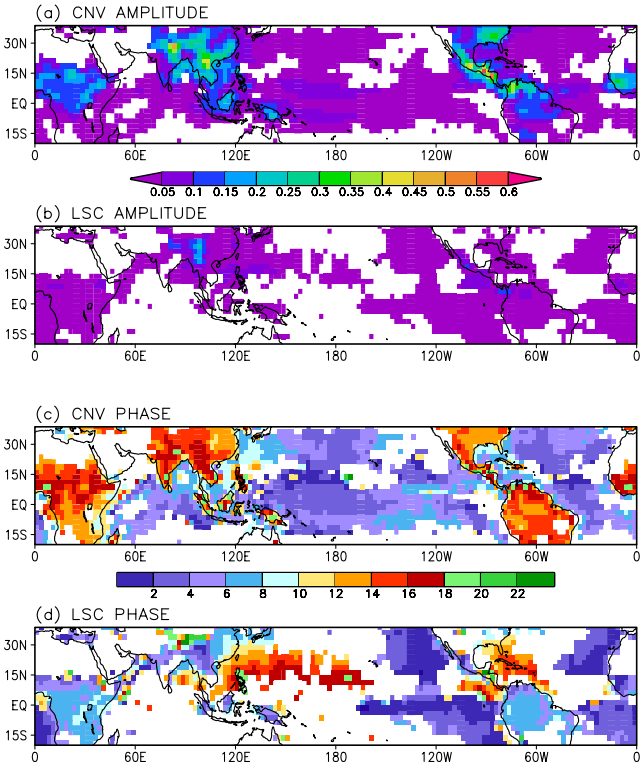

Figure 5. Amplitudes (mm h^{-1}) and maximum phases (LST) of the diurnal cycle of convective (CNV) and stratiform (LSC) precipitation in the AMIP simulation.

(Figures 7 and 8). The diurnal amplitudes in the CTRL run are comparable with those from the AMIP run (compare Figures 7a and 2b). There are no systematic differences in the maximum phases (compare Figures 8a and 3b). This indicates that the phase is not affected much by the differences in the SST conditions or different sampling. Even though the model was integrated for just one summer with climatological SSTs, the results suggest that the global pattern of the diurnal cycle, especially the phase, is quite robust.

[29] The increase of the RAS relaxation timescale in EXP2 (Figure 7c) and EXP3 (Figure 7d) results in a significant reduction in the amplitude both over the continents and oceans. Particularly in EXP2, the reduction in amplitude is quite substantial over much of the continents and the adjacent oceans, consistent with the findings of *Lin et al.* [2000]. In the global (20°S–40°N) composites over land (not shown), the amplitude of the diurnal cycle is reduced by more than 50% in EXP2 and 30% in EXP3 compared with the CTRL. In contrast, the change in the convection starting level increased the amplitude in most regions, with about a 20% increase in the global mean.

[30] The change in the convection starting level (EXP1 in Figure 8b) tends to slightly delay the phase of the maximum by 1–3 hours, mostly over the continents. When the relaxation timescale is increased (EXP2 in Figure 8c), the geographical distribution of the phase is less organized and more widely varying over the continent. In EXP2 there are many areas over the continents where the diurnal cycle is undefined (i.e., statistically not significant), apparently affected by the substantial reduction in diurnal amplitudes. However, the number of grid points that have an evening to nighttime maximum tends to increase in EXP2, showing significant delays in time from the CTRL experiment.

[31] Despite the reduction in amplitude, EXP3 (Figure 8d) in general shows an improved simulation of the precipitation diurnal cycle especially in terms of the phase over the continents. In particular, the run tends to capture the late afternoon maxima over the eastern United States and central South America. It also appears to reproduce the late evening to nighttime precipitation maxima over the eastern slope of the Rocky Mountains, Central America, northern South America, and the Maritime Continent. The maxima over the southern flanks of the Tibetan Plateau also show nocturnal peaks, consistent with the TRMM patterns shown in Figure 3a. On the other hand, the phases over the ocean have not changed much. This is especially true for the subtropical ocean where the model is quite dry. However, the phases of the maxima are delayed and closer to the observations over the adjacent oceans, presumably affected by the improved simulation in phase over the land. This includes for example, the Bay of Bengal, the South China Sea, and the Gulf of Mexico.

[32] We further compare the simulated and observed time evolutions of precipitation averaged over several selected regions where the diurnal cycle is distinct (Figure 9). We filter the time series (filtering out the cycles shorter than 12 hours) in order to provide a clearer picture of the systematic changes in the amplitude and maximum phase among the sensitivity experiments. It turns out that the filtered values provide a fairly good approximation to the full seasonal mean (June–August) diurnal time series. As discussed earlier, EXP3 exhibits improved simulations of

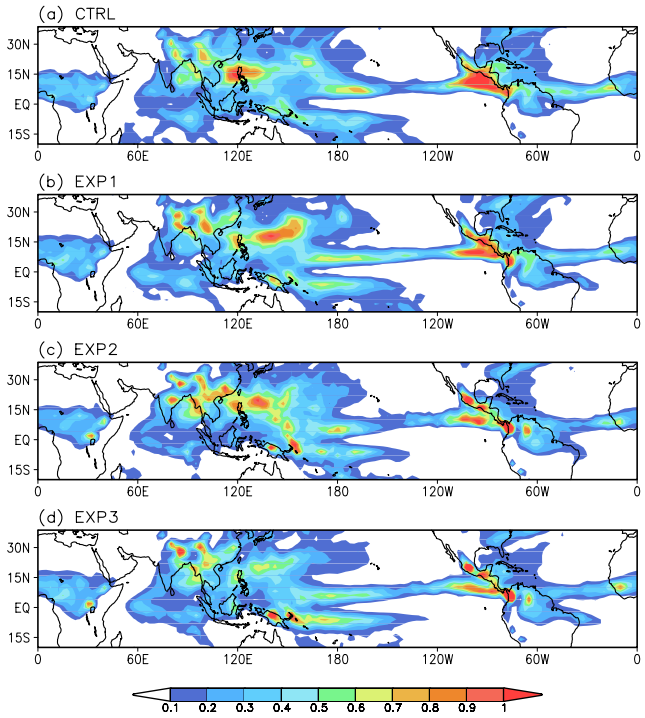

Figure 6. Horizontal distributions of summer mean (June–August) precipitation (mm h^{-1}) from the (a) CTRL (control), (b) EXP1, (c) EXP2, and (d) EXP3 runs.

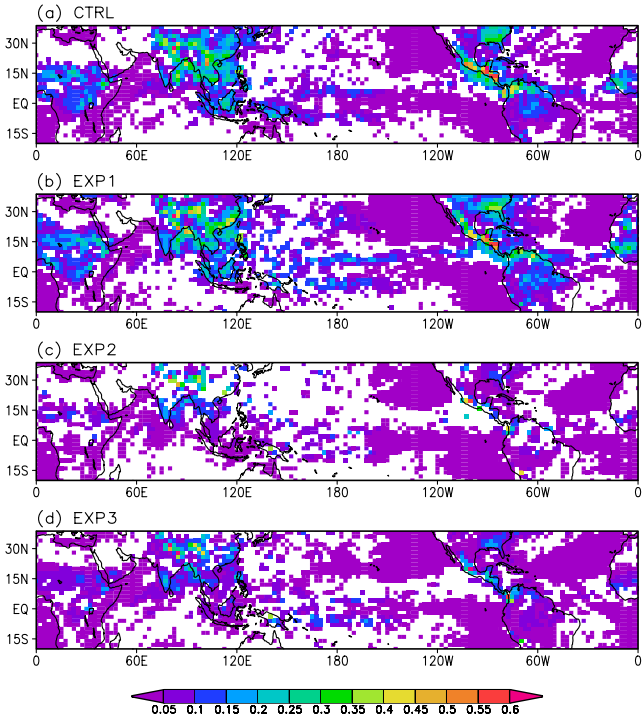

Figure 7. Amplitudes of the diurnal cycle of precipitation (mm h^{-1}) from the (a) CTRL, (b) EXP1, (c) EXP2, and (d) EXP3 runs. Only the grid points with an amplitude that is significant at the 10% level are shaded.

the phase of the maximum of diurnal precipitation in most regions. The western Pacific is an exception to this, where the modifications to the convection scheme only affect the seasonal mean precipitation. There is also a regional dependence on the amplitude changes. The decrease in amplitude in EXP3 helps reduce the strong amplitude biases in the CTRL run over the eastern United States, the East Asian monsoon and the Indian monsoon regions. However, the amplitude reduction is too strong in the North American monsoon region. The relatively weak signal of the semidiurnal component in the model simulation seems to be another problem, for example over the East Asian monsoon region and the western Pacific.

[33] Comparing the changes in the maximum phase in terms of histograms (Figure 10), the timing of the maximum over land is significantly shifted with respect to the CTRL by 2 hours (to 1600 LST) in EXP1, and 3 hours (to 1700 LST) in EXP3 in a global mean sense. This brings the distributions from those experiments closer to the observed distributions (compare Figure 4a). The distribution over ocean changes little among the sensitivity runs, with a peak probability at 0200 LST. This peak is in fact 2 hours earlier than that in the AMIP run. This discrepancy seems to be caused by smaller sampling over the subtropical dry oceans in the climatological SST runs that consist of just one season integration (compare Figures 3b and 8a).

4.2. Diurnal Cycles of MSE and CAPE

[34] In this section we look further into the mechanisms of the diurnal cycle of precipitation and how the modifications to the convection scheme affect it. Figure 11 shows the control experiment's diurnal variations of MSE (h) averaged over land and ocean (Figures 11a and 11b), along with the diurnal departures from the daily mean values (Figures 11c and 11d). There are fundament differences in the diurnal variation of MSE between land and ocean, suggesting differences in the diurnal convection mechanism. In view of the strong daytime surface heating and nighttime cooling, the model simulates a much stronger diurnal variation over the land than over the ocean, with an amplitude that is several times larger in the boundary layer. The composite diurnal cycle of h over land shows the daytime development of the atmospheric boundary layer up to 800 hPa level. Note that the evolution of h shows a vertically tilted structure within the boundary layer (delayed in time from the ground), indicating upward energy transport from the ground. At higher levels above the boundary layer, the vertical tilt disappears, reflecting a direct radiative cooling and heating of the atmosphere during the day. Although less prominent, the diurnal variation of the oceanic boundary layer can be seen also, with a shallower vertical depth compared to the land. Unlike for the land, the middle and upper level variability of h seems to be important over the ocean.

[35] As a measure of convective instability, we calculated the vertical profiles of energy difference between the surface MSE (h_p) and the saturated MSE (h^*) of the environment (Figures 11e and 11f). The difference represents the buoyancy when the parcel is lifted adiabatically from the ground, and its vertical integration is equivalent to CAPE. The results just give a qualitative picture of the vertical structure of convective buoyancy and its diurnal variation, since the estimates are from spatially averaged profiles. In the convectively unstable case, the buoyancy changes its sign from

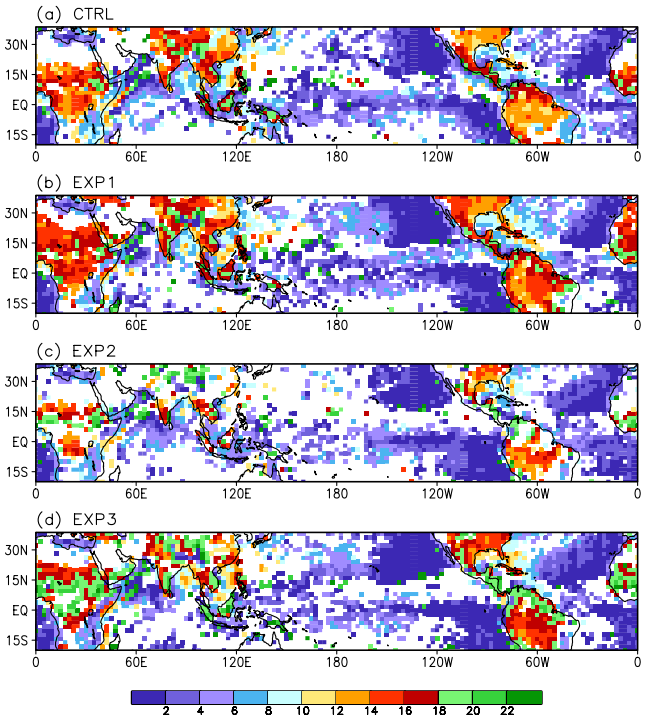

Figure 8. Same as in Figure 7 except the maximum phases of the diurnal cycle of precipitation (LST).

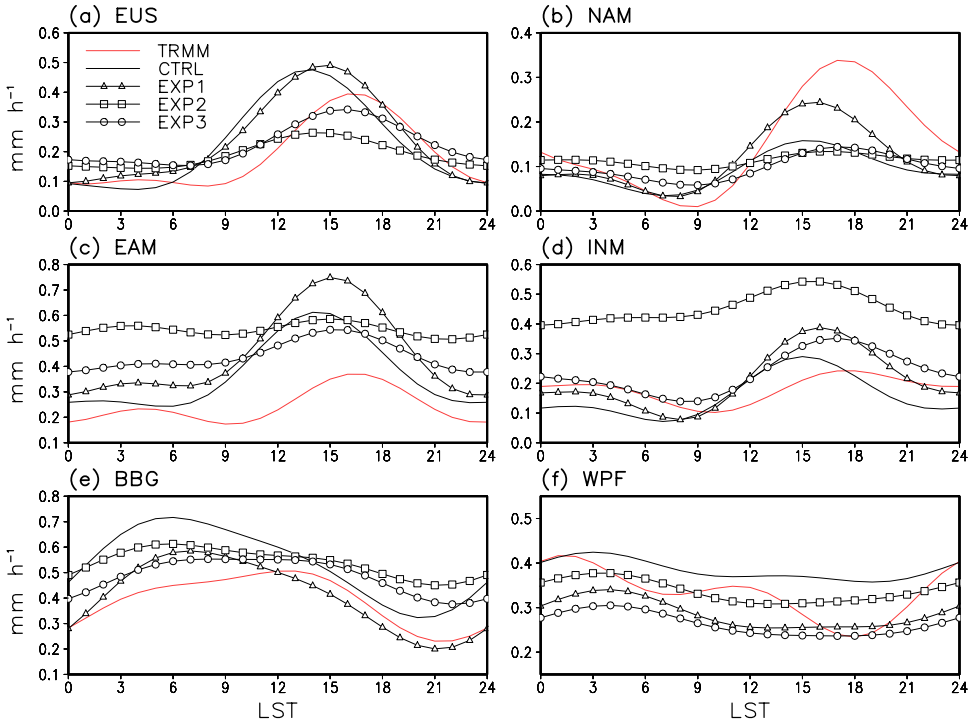

Figure 9. Time mean diurnal variations of precipitation (mm h^{-1}) over the (a) eastern United States (90–75°W, 30–40°N), (b) the North American monsoon region (115–100°W, 22–35°N), (c) the East Asian monsoon region (105–120°E, 20–30°N), (d) the Indian monsoon region (72.5–82.5°E, 10–20°N), (e) the Bay of Bengal (85–95°E, 10–20°N), and (f) the western Pacific (130–145°E, 0–10°N) from TRMM and the four climatological SST runs. The cycles shorter than 12-hour period were filtered out in each time series using a harmonic filter. Only the land points are averaged for Figures 9a–9d, and only the ocean points are averaged for Figures 9e–9f.

negative to positive at the level of free convection (LFC), and changes again to negative values at the neutral buoyancy level (NBL) where h_p equals h^*. The integration of negative buoyancy from the ground up to the LFC represents the convective inhibition (CIN).

[36] The diurnal variation of $h_p - h^*$ clearly shows the amplification of CAPE in the day over land. The positive buoyancy layer between the LFC and the NBL expands to its maximum depth at 1500 LST, which is roughly the peak time of diurnal precipitation over land in the model. The CIN reaches to its diurnal minimum during this time. From midnight to early morning, no positive buoyancy layer is defined in the vertical, indicating a suppression of convection.

[37] Over ocean, the model tends to produce positive buoyancy layers during most of the day. However, relatively larger buoyancy is generated in the nighttime, which could explain the nocturnal peak of oceanic diurnal precipitation. This suggests that, unlike for land convection, oceanic convection is less tied to the boundary layer heating and more influenced by upper atmospheric variations. This process does not seem to be unrealistic in the tropical ocean, where for example, nocturnal longwave emission of moisture and high clouds acts to decrease the vertical stability [*Sui et al.*, 1997; *Randall et al.*, 1991; *Woolnough et al.*, 2004]. Although the current model has no diurnal variations in the prescribed SSTs, the tendency of nocturnal precipitation in the atmosphere-ocean coupled case should not be qualitatively different [*Dai and Trenberth*, 2004], considering the higher heat capacity of the ocean with an ocean mixed layer.

[38] To help validate the vertical structure of the model simulations, we compare in Figure 12 the observed and simulated diurnal variations of the MSE over the four IOP regions where special sounding observations are available through various field experiments (NAME, ARM, GATE, and TOGA COARE). Although the observations have a more limited sampling in time (3 hour interval in ARM and GATE, and 6 hour in NAME and TOGA COARE), the comparison suggests that the model simulations are realistic in the diurnal phases. The model basically captures the observed variation of the PBL over land (the NAME and ARM cases), with a vertically tilted structure. The model simulations are also reasonable over ocean (the GATE and TOGA COARE cases), where the upper level diurnal variations become as strong as in the boundary layer. However, the model simulates noticeable differences in the lower levels, probably due to the prescribed SST which do not have a diurnal variation. The diurnal variations in $h_p - h^*$ profile are also consistent between the observations and the model, displaying a daytime maxima of CAPE over land, and nighttime maxima over ocean (not shown).

[39] Given the vertically tilted structure of h in the PBL, the timing of the maximum convection (precipitation) over land may be substantially influenced by the definition of the convection starting level. Figure 13 compares the diurnal

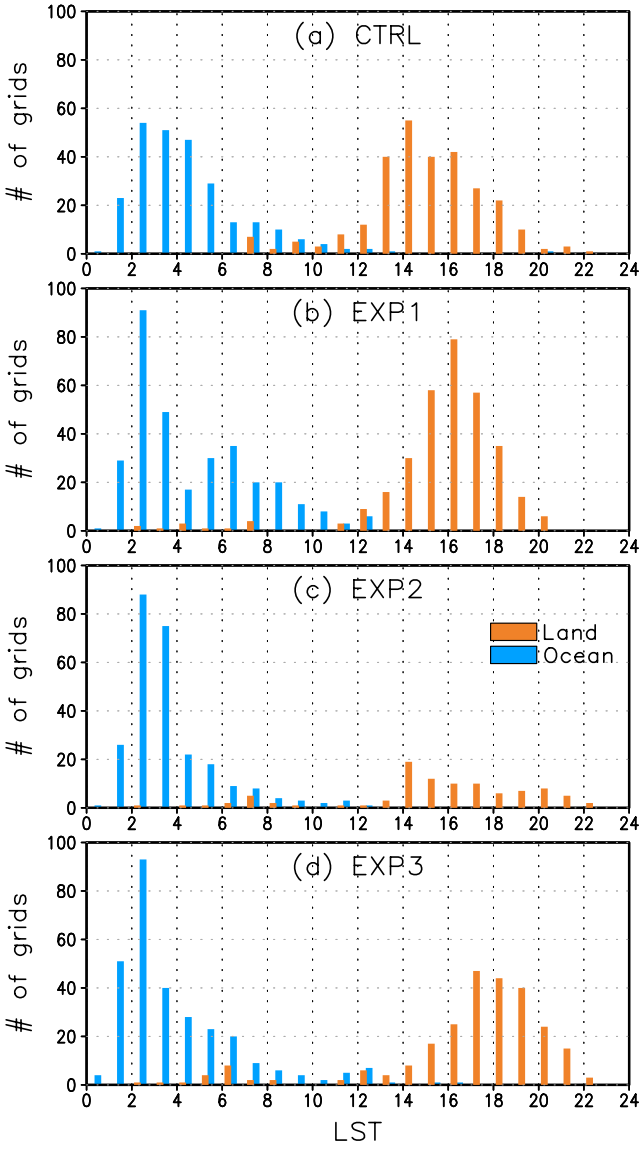

Figure 10. Histograms of the maximum phases in the diurnal cycle of precipitation in (a) CTRL, (b) EXP1, (c) EXP2, and (d) EXP3. Others are same as in Figure 4.

variation of CAPE in the CTRL and EXP2 runs. Comparing the case when the convection starting level for the CAPE calculation in the CTRL run is chosen above the lowest two levels (solid line), with the case when the convection starting level is chosen above the lowest 10 levels (short-dashed line), the timing of peak CAPE is delayed by several hours in the latter case. This is consistent with the phase delay in the diurnal peak timing of precipitation between CTRL and EXP1 runs. The diurnal amplitude of CAPE becomes smaller in the case of a higher convection starting level. This is because this model uses the PBL-averaged MSE for the energy of the lifted parcel, which must be smaller than the near-ground MSE. In this regard, it is not clear why the diurnal amplitude of land precipitation in EXP1 increased from that of the CTRL (compare Figure 7). Over ocean, the lifting of the convection starting level also tends to shift the maximum phase of CAPE to early morning, although the peak time in the diurnal precipitation is not so evident in Figure 8.

[40] Although less substantial, the increase in the relaxation timescale (long-dashed line in Figure 13) also induces a delay in the phase for the diurnal variation of CAPE, both over land and ocean. It appears that the increase in the relaxation timescale introduces an initial reduction of precipitation intensity due to the partial adjustment of large-scale instability. In this case, the CAPE decays more slowly to increase the lifetime of convection.

5. Summary

[41] The characteristics of the diurnal cycle of warm-season precipitation and their sensitivity to the modifications in the convection parameterization were examined in simulations with the NASA/NSIPP AGCM. TRMM TMI satellite rainfall estimates for the period 1998–2004 were used for validation. The AMIP-style model integrations were done at a horizontal resolution of 2° by 2.5° (latitude by longitude) and forced with the observed SSTs for the TRMM period.

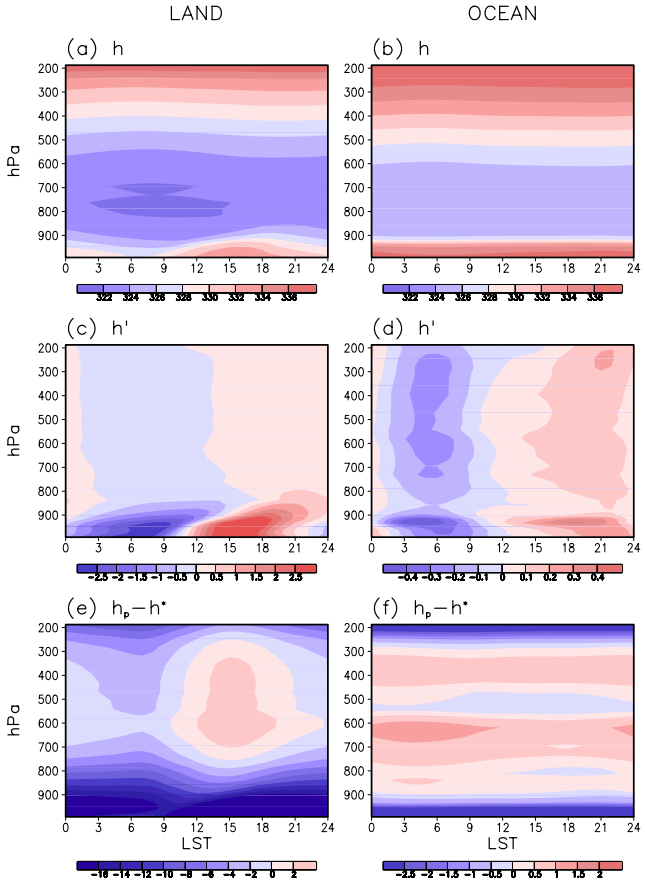

Figure 11. Diurnal variations of the moist static energy (h) profile in (a) land and (b) ocean. (c and d) Diurnal departures of h when the daily mean values are subtracted in each level. (e and f) Vertical profiles of the surface moist static energy (h_p) minus saturated moist static energy (h^*) of environment. The averaged values in the lowest two model levels are used for h_p. The unit is kJ kg^{-}1.

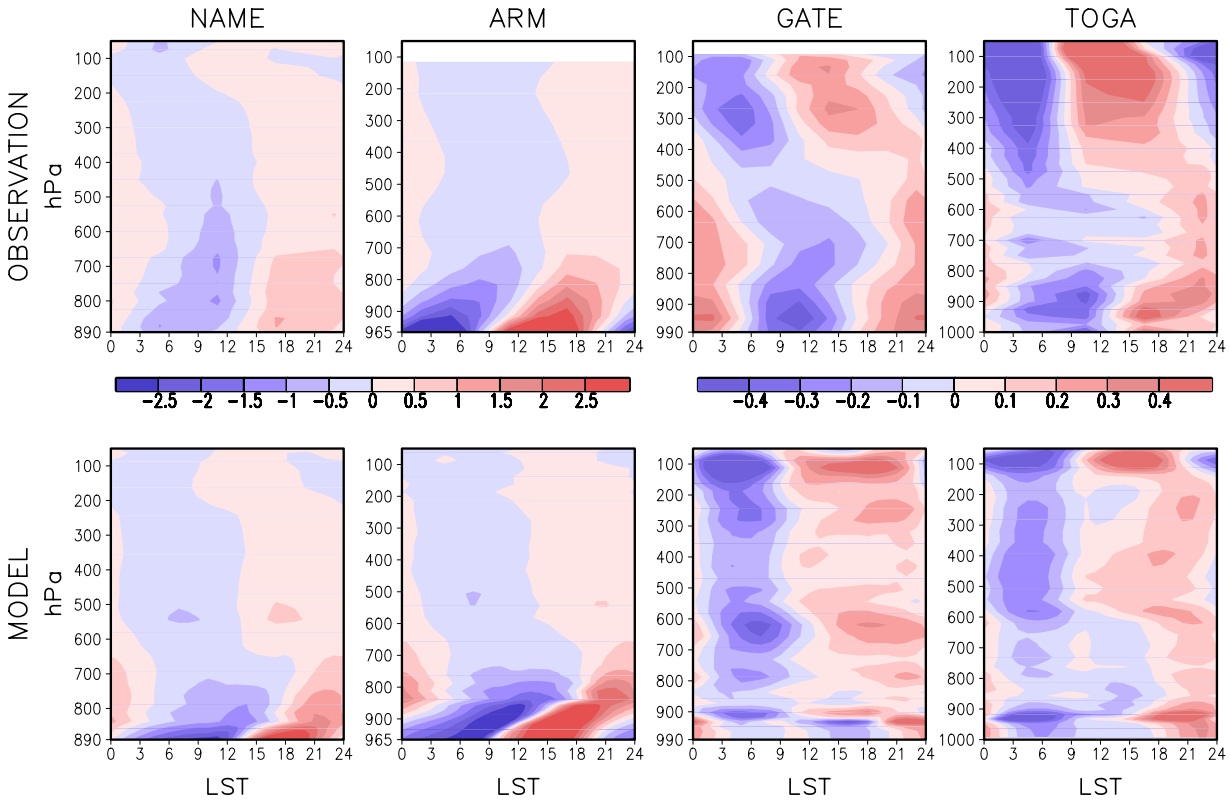

Figure 12. Diurnal variations of the MSE over the four IOP regions from (top) the observations and (bottom) the CTRL run. Time mean values are subtracted in each figure. The unit is kJ kg^{-1}.

[42] Although the model captures the basic characteristics of the diurnal cycle over land (daytime maximum) and ocean (nighttime maximum), there are several prominent discrepancies, especially in the phase. Over land, the model tends to simulate the maximum precipitation in the early afternoon (most at 1400 LST), which is several hours earlier than the observed evening maximum (1800 LST). In addition, the probability of peak timing is more locked to the afternoon hours, and the model produces too little precipitation in the nighttime over land. Similar phase errors (maximum is biased early) can be found over ocean, although the observed and model statistics of the diurnal cycle are less robust. The total precipitation is predominantly made up of convective precipitation, and its diurnal variation is mostly governed by convective precipitation, both over land and ocean. This implies that deficiencies in the deep convection scheme of the model are the primary cause of the incorrect representation of the diurnal cycle.

[43] Two modifications to the RAS convection scheme were tested to examine their influences on the amplitude and phase of the diurnal cycle of precipitation. It was found that changes in the convection starting level and in the relaxation timescale each led to improvements in the diurnal cycle of precipitation, especially in correcting the phase errors over land. A run with both modifications to the convection scheme produced results closest to the TRMM observations.

[44] The mechanisms that drive the changes in the diurnal cycle of precipitation in the modified convection schemes were examined by analyzing the vertical structure of the MSE and CAPE. The diurnal variation in the MSE profile showed characteristic land-ocean differences. While the convection over land is predominantly forced by daytime PBL heating, convection over ocean is substantially influenced by nocturnal radiative cooling in the free atmosphere. This makes the diurnal variation of CAPE out of phase between land and ocean. The diurnal variation of the simulated precipitation varies coherently with that of CAPE,

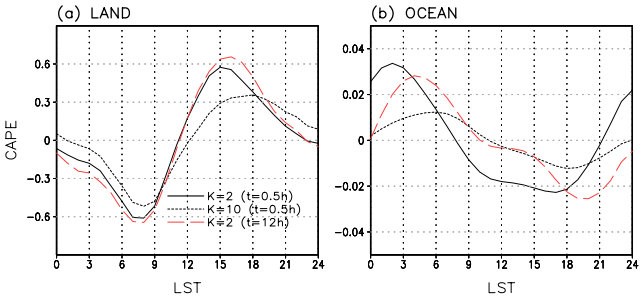

Figure 13. Diurnal variations of CAPE (kJ kg^{-1}) over (a) land and (b) ocean for three different cases. The two black lines show the CAPE calculated from the CTRL run (relaxation timescale is 0.5 hours) with the convection starting level set to the 2nd (solid), and 10th (short dash) model layers from the surface. The long dashed line (red) indicates the case where CAPE is calculated from the EXP2 run, which has a relaxation timescale of 12 hours. Daily mean is subtracted in each time series.

and accordingly shows an out of phase relationship in the diurnal maximum between land and ocean. These characteristic differences between land and ocean in the model were verified with the observed sounding data sets from the four field experiments.

[45] As a result of the upward transport of heat and moisture from the ground, the moist static energy in the PBL over land shows a vertically tilted structure during the day time, and a resulting delay in the phase of the maximum in the MSE at higher levels. Those results suggest that the timing of maximum convection should be much influenced by the definition of the convection starting level. In particular, when the convection scheme uses a higher starting level such as is effectively the case when the lifted parcel is initiated with the PBL mean moist static energy, the timing of the maximum CAPE and the precipitation is delayed by several hours.

[46] The increase in the relaxation timescale induces a similar delay in the timing of the maximum CAPE. In this case, we speculate that the increase in the relaxation timescale introduces an initial reduction in the precipitation intensity due to the partial adjustment of large-scale instability, by which the CAPE could slowly decay at a longer timescale. This would increase the convection lifetime and delay the maximum phase in deep convection.

[47] Although our modifications to the convection scheme showed improvements in the simulations of the diurnal cycle, our purpose for doing the sensitivity experiments was primarily to gain a better understanding of the different mechanisms that produce the diurnal cycle in current models, and how those might be improved in future models. In fact, those improvements were far from perfect and were to a large extent limited to correcting the phase biases over the continents. The modifications brought unrealistically weak amplitudes in the simulated diurnal cycle of precipitation, which is mainly driven by the increase of the relaxation timescale. This result is somewhat consistent with the findings by *Pan and Randall* [1998] and *Lin et al.* [2000], in that the increase of the relaxation timescale suppresses deep convection too much in the model. The strong sensitivity of the model nevertheless provides important implications on modeling the amplitudes of the diurnal cycle. In fact, our control simulations with a timescale of 0.5 hours produced relatively stronger amplitude biases compared with the TRMM observations (with an unrealistically high ratio of convective precipitation). This implies that 0.5 hours might be too short for the given range of the value (as discussed in section 2), and a more vigorous sensitivity test to the timescale is required. We carried out further experiments (not shown) in which we changed the timescale to intermediate values (τ = 1, 2, and 6 hours), and found that the amplitude of the diurnal cycle decreased monotonically with an increase in the timescale, mostly over the continents. On the other hand, the phase changes were more or less limited (saturated) to a 1–3 hour delay from the control run, with a timescale of a few hours.

[48] In summary, the results of this study suggest that a better representation of the diurnal cycle of precipitation can be achieved by improving the simulation of moist convection. This should include improvements in the interaction with the PBL, the characteristic timescale of the convection adjustment, and the triggering process for nocturnal precipitation.

[49] **Acknowledgments.** We are grateful to Paul Ciesielski for providing the sounding observation data sets that we used in this study. We thank Julio Bacmeister, Xin Lin, and three anonymous reviewers for their helpful comments on the manuscript. This study was supported by NOAA's Climate Prediction Program for the Americas (CPPA) and NASA's Modeling, Analysis, and Prediction (MAP) program.

References

Arakawa, A., and W. H. Schubert (1974), Interaction of a cumulus cloud ensemble with the large-scale environment, Part I, *J. Atmos. Sci.*, *31*, 674–699.

Arakawa, A., and M. J. Suarez (1983), Vertical differencing of the primitive equations in sigma coordinates, *Mon. Weather Rev.*, *111*, 34–45.

Bacmeister, J. T., P. J. Pegion, S. D. Schubert, and M. J. Suarez (2000), Atlas of seasonal means simulated by the NSIPP 1 atmospheric GCM, *NASA Tech. Memo.*, *17*, 194 pp.

Bell, T. L., and N. Reid (1993), Detection of the diurnal cycle of tropical rainfall from satellite observations, *J. Appl. Meteorol.*, *32*, 311–322.

Bell, T. L., P. K. Kundu, and C. Kummerow (2001), Sampling errors of SSM/I and TRMM rainfall averages: Comparison with error estimates from surface data and a simple model, *J. Appl. Meteorol.*, *40*, 938–954.

Bowman, K. P., J. C. Collier, G. R. North, Q. Wu, E. Ha, and J. Hardin (2005), The diurnal cycle of tropical precipitation in Tropical Rainfall Measuring Mission (TRMM) satellite and ocean buoy rain gauge data, *J. Geophys. Res.*, *110*, D21104, doi:10.1029/2005JD005763.

Carbone, R. E., J. D. Tuttle, D. A. Ahijevych, and S. B. Trier (2002), Inferences of predictability associated with warm season precipitation episodes, *J. Atmos. Sci.*, *59*, 2033–2056.

Chen, M., R. E. Dickinson, X. Zeng, and A. N. Hahmann (1996), Comparison of precipitation observed over the continental United States to that simulated by a climate model, *J. Clim.*, *9*, 2233–3349.

Chou, M.-D., and M. J. Suarez (1994), An efficient thermal infrared radiation parameterization for use in general circulation models, *NASA Tech. Memo.*, *3*, 85 pp.

Chou, M.-D., M. J. Suarez, C.-H. Ho, M. M.-H. Yan, and K.-T. Lee (1998), Parameterizations for cloud overlapping and shortwave single-scattering properties for use in general circulation and cloud ensemble models, *J. Clim.*, *11*, 202–214.

Ciesielski, P. E., R. H. Johnson, P. T. Haertel, and J. Wang (2003), Corrected TOGA COARE sounding humidity data: Impact on diagnosed properties of convection and climate over the warm pool, *J. Clim.*, *16*, 2370–2384.

Collier, J. C., and K. P. Bowman (2004), Diurnal cycle of tropical precipitation in a general circulation model, *J. Geophys. Res.*, *109*, D17105, doi:10.1029/2004JD004818.

Collier, J. C., and G. J. Zhang (2006), Simulation of the North American monsoon by the NCAR CCM3 and its sensitivity to convection parameterization, *J. Clim.*, *19*, 2851–2866.

Dai, A. (2006), Precipitation characteristics in eighteen coupled climate models, *J. Clim.*, *19*, 4605–4630.

Dai, A. G., and K. E. Trenberth (2004), The diurnal cycle and its depiction in the Community Climate System Model, *J. Clim.*, *17*, 930–951.

Dai, A. G., F. Giorgi, and K. E. Trenberth (1999), Observed and model-simulated diurnal cycles of precipitation over the contiguous United States, *J. Geophys. Res.*, *104*, 6377–6402.

Johnson, R. H., P. E. Ciesielski, B. D. McNoldy, P. J. Rogers, and R. K. Taft (2007), Multiscale variability of the flow during the North American Monsoon Experiment, *J. Clim.*, *20*, 1628–1648.

Koster, R. D., and M. J. Suarez (1996), Energy and water balance calculations in the Mosaic LSM, *NASA Tech. Memo.*, *9*, 194 pp.

Kummerow, C., et al. (2000), The status of the Tropical Rainfall Measuring Mission (TRMM) after two years in orbit, *J. Appl. Meteorol.*, *39*, 1965–1982.

Lee, M. I., S. D. Schubert, M. J. Suarez, I. M. Held, N. C. Lau, J. J. Ploshay, A. Kumar, H. K. Kim, and J. K. E. Schemm (2007a), An analysis of the warm-season diurnal cycle over the continental United States and northern Mexico in general circulation models, *J. Hydrometeorol.*, *8*, 344–366.

Lee, M. I., et al. (2007b), Sensitivity to horizontal resolution in the AGCM simulations of warm season diurnal cycle of precipitation over the United States and northern Mexico, *J. Clim.*, *20*, 1862–1881.

Liang, X.-Z., L. Li, A. Dai, and K. E. Kunkel (2004), Regional climate model simulation of summer precipitation diurnal cycle over the United States, *Geophys. Res. Lett.*, *31*, L24208, doi:10.1029/2004GL021054.

Lin, X., D. A. Randall, and L. D. Fowler (2000), Diurnal variability of the hydrological cycle and radiative fluxes: Comparisons between observations and a GCM, *J. Clim.*, *13*, 4159–4179.

Louis, J., M. Tiedtke, and J. Geleyn (1982), A short history of the PBL parameterization at ECMWF, paper presented at Workshop on Planetary Boundary Layer Parameterization, Eur. Cent. for Med.-Range Weather Forecasting, Reading, U. K.

Moorthi, S., and M. J. Suarez (1992), Relaxed Arakawa-Schubert: A parameterization of moist convection for general circulation models, *Mon. Weather Rev.*, *120*, 978–1002.

Nesbitt, S. W., and E. J. Zipser (2003), The diurnal cycle of rainfall and convective intensity according to three years of TRMM measurements, *J. Clim.*, *16*, 1456–1475.

Olson, W. S., C. D. Kummerow, S. Yang, G. W. Petty, W. K. Tao, T. L. Bell, S. A. Braun, Y. Wang, S. E. Lang, D. E. Johnson, and C. Chiu (2006), Precipitation and latent heating distributions from satellite passive microwave radiometry. Part I: Improved method and uncertainties, *J. Appl. Meteorol. Climatol.*, *45*, 702–720.

Pan, D.-M., and D. A. Randall (1998), A cumulus parameterization with a prognostic closure, *Q. J. R. Meteorol. Soc.*, *124*, 949–981.

Randall, D. A., and D. A. Dazlich (1991), Diurnal variability of the hydrological cycle in a general circulation model, *J. Atmos. Sci.*, *48*, 40–62.

Reynolds, R. W., N. A. Rayner, T. M. Smith, D. C. Stokes, and W. Wang (2002), An improved in situ and satellite SST analysis for climate, *J. Clim.*, *15*, 1609–1625.

Riley, G. T., M. G. Landin, and L. F. Bosart (1987), The diurnal variability of precipitation across the Central Rockies and adjacent Great Plains, *Mon. Weather Rev.*, *115*, 1161–1172.

Schumacher, C., and R. A. Houze (2003), Stratiform rain in the tropics as seen by the TRMM precipitation radar, *J. Clim.*, *16*, 1739–1756.

Suarez, M. J., and L. L. Takacs (1995), Documentation of the Aries-GEOS dynamical core: Version 2, *NASA Tech. Memo.*, *10*, 56 pp.

Sui, C.-H., K.-M. Lau, Y. N. Takayabu, and D. A. Short (1997), Diurnal variations in tropical oceanic convection during TOGA COARE, *J. Atmos. Sci.*, *54*, 639–655.

Woolnough, S. J., J. M. Slingo, and B. J. Hoskins (2004), The diurnal cycle of convection and atmospheric tides in an aquaplanet GCM, *J. Atmos. Sci.*, *61*, 2559–2573.

Yang, G. Y., and J. Slingo (2001), The diurnal cycle in the tropics, *Mon. Weather Rev.*, *129*, 784–801.

Zhang, G. J. (2003), Roles of tropospheric and boundary layer forcing in the diurnal cycle of convection in the U. S. southern Great Plains, *Geophys. Res. Lett.*, *30*(24), 2281, doi:10.1029/2003GL018554.

Zhang, M. H., J. L. Lin, R. T. Cederwall, J. J. Yio, and S. C. Xie (2001), Objective analysis of ARM IOP data: Method and sensitivity, *Mon. Weather Rev.*, *129*, 295–311.

T. L. Bell, K.-M. Kim, M.-I. Lee, S. D. Schubert, and M. J. Suarez, Global Modeling and Assimilation Office, Code 610.1, NASA Goddard Space Flight Center, Greenbelt, MD 20771, USA. (milee@gmao.gsfc.nasa.gov)